

Environmentally friendly polymeric films based on biocarbon, synthetic zeolite and PVP for agricultural chemistry

Citation

VAŇHAROVÁ, Ludmila, Markéta JULINOVÁ, Martin JURČA, Antonín MINAŘÍK, Štěpán VINTER, Dagmar ŠAŠINKOVÁ, and Erik WRZECIONKO. Environmentally friendly polymeric films based on biocarbon, synthetic zeolite and PVP for agricultural chemistry. *Polymer Bulletin* [online]. Springer Science and Business Media Deutschland, 2021, [cit. 2023-03-31]. ISSN 0170-0839. Available at <https://link.springer.com/content/pdf/10.1007/s00289-021-03765-z.pdf>

DOI

<https://doi.org/10.1007/s00289-021-03765-z>

Permanent link

<https://publikace.k.utb.cz/handle/10563/1010363>

This document is the Accepted Manuscript version of the article that can be shared via institutional repository.

Environmentally friendly polymeric films based on biocarbon, synthetic zeolite and PVP for agricultural chemistry

Ludmila Vaňharová¹, Markéta Julinová¹, Martin Jurča¹, Antonín Minařík², Štěpán Vinter¹, Dagmar Šašínková¹, Erik Wrzecionko²

¹Department of Environmental Protection Engineering, Faculty of Technology, Tomas Bata University in Zlin, Vavreckova 275, 760 01 Zlin, Czech Republic

²Department of Physics and Material Engineering, Faculty of Technology, Tomas Bata University in Zlin, Vavreckova 275, 760 01 Zlin, Czech Republic

*Markéta Julinová julinova@utb.cz

Abstract

An investigation was made into polymeric films based on polyvinylpyrrolidone (PVP) as the matrix, in combination with synthetic zeolite and dried or pyrolyzed biocarbon (biochar). The films were prepared by the casting method, and their properties were variously analysed (optical microscopy, FTIR analysis, differential scanning calorimetry, mechanical properties, water solubility, water uptake). Evaluation also encompassed the biological decomposition of the films in the soil environment and their influence on the growth of *Sinapis alba*. Optical microscopy indicated the particles of the fillers were almost completely evenly distributed in the polymer matrix, therein forming networks randomly. Since the space between the particles decreased as particle content increased, raising the content of the fillers brought about more compact networks. The IR spectra for the films proved the occurrence of hydrogen bonding between the PVP and synthetic zeolite. The processing and mechanical properties of the prepared polymeric films were acceptable. Water solubility and the water uptake of the films were satisfactory regarding handling and further use. Respirometric tests indicated a positive effect by the biocarbon on the biodegradation of the tested films. The proposed combination of synthetic zeolite and biocarbon fillers positively influenced the germination rate of *Sinapis alba*, while the polymer matrix (PVP) did not hinder further growth. Observations and testing led to the conclusion that the materials based on PVP with fillers (synthetic zeolite/ biocarbon) have the potential for agricultural utilization.

Keywords: Polyvinylpyrrolidone, biochar, synthetic zeolites, biocarbon, biodegradation, *sinapis alba*

Introduction

Several issues have arisen in recent decades relating to polymeric materials, such as limited petroleum resources, the greenhouse effect caused by unrestricted carbon emissions into the atmosphere by industry at large and the poor biodegradability demonstrated by materials accumulating in the natural environment [1]. A new trend in research has emerged in response, with the aim of devising materials based on renewable resources or incorporating naturally occurring additives into a synthetic polymer that forms the matrix. Natural fillers appear to be a good alternative to synthetic options, due to their low cost, environmentally friendly properties and biodegradability. A material containing at least one fully biodegradable component is often referred to as a “biocomposite” for medicinal applications or

a “green composite” for environmental ones [2]. Contemporary research tends to focus on enhancing their properties and development [3].

Mohanty et al. [4] and Nesić et al. [5] state that polyvinylpyrrolidone (PVP) constitutes a possible option for the matrix of such biocomposites or green composites. This linear-chained amorphous polymer is soluble in water and is known for its unique physical-chemical properties, as well as low toxicity. This makes it applicable for biomedicine, pharmaceuticals, cosmetics, detergents and agricultural chemistry (“agro-chemistry”).

PVP is not suitable for thermoplastic processing in the usual manner since it is very brittle in pure form, which is why plasticizers are added to make PVP-based films [6, 7]. A recent shift has been to utilize natural or biodegradable plasticizers with low toxicity and good compatibility [8]; examples compatible with PVP and water include glycerol, sorbitol, mannitol, arabic gum, polyethylene and glycol [9-11]. One in widespread use is glycerol, a highly hygroscopic molecule usually added to film-forming solutions to prevent brittleness in the resultant material [8]. Gum arabic is an appealing choice with the benefit of being quite cheap. It is a polysaccharide obtained from the sap of certain species of acacia; it is applied in the cosmetics, food and pharmaceuticals industries for its numerous physical and rheological properties [12]. The use of water as a solvent can be crucial, inasmuch as it plays a significant role as a plasticizer for PVP systems [9].

Fillers (inorganic and organic) acting as composites employed in a method for water-soluble polymeric processing have the capability of affecting the final mechanical properties of the material to a notable extent, either positively or negatively, as well as its rate of biodegradability. The intention of applying a filler with a positive effect is to improve the dimensional stability, hardness, strength, resistance to abrasion, thermal stability of materials and electroconductivity [13-16]. Description has even been given of organic-inorganic hybrid composites [17]. For example, Alver et al. [18] studied composites based on PVP/chitosan and zeolite created by solution blending. They positively evaluated the zeolites (aluminosilicates with threedimensional framework structures) as they possessed numerous interesting chemical and physical properties. The author concluded that the combination of PVP and said zeolites improved the thermal stability and mechanical properties of chitosan in the comparison with the pure form.

Biochar is an example of a very interesting filler [19-24], and biomass pyrolysis, as a means for generating renewable resources, has become popular in contemporary research. The natural waste material is processed, and the resulting product, if deemed suitable and harmless, enriches the soil with important elements [25, 26]. Chen et al. [27] investigated biochar as a filler for a polymeric material of polyvinyl alcohol/PVP. Therein, research was conducted on preparing and characterizing a material that could encapsulate the fertilizer and facilitate gradual release. The authors stated the presence of biochar heightened both the resistance of the material to water and its biodegradability in soil. Biodegradation assessed by weight loss reached 33% after 120 days, which is notable since polyvinyl alcohol and PVP prove difficult to decompose in the soil environment [28].

Subsequent studies have tested other organic additives of natural origin [14, 17], such as banana [29] or bamboo [30] fibre, date leaves [4] and chicken feathers [31, 32]. There has also been a rise in the utilization of non-recyclable agricultural waste, e.g. cow or poultry dung, in concrete [33-39]. For example, Yusefi et al. [35] tested green composites based on polylactic acid, wherein cow manure acted as a form of reinforcement. Apart from containing proteins, hemicelluloses and cellulose, it is also rich in elements and completely biodegradable. The cow dung in the aforementioned study brought about an improvement in mechanical properties—in flexural, tensile and impact strengths.

This study deals with preparing PVP-based, water-soluble polymeric films applicable for agro-chemistry, e.g. for seed encapsulation, and hence the choice of biocarbon for the main component. The secondary component comprised a synthetically prepared zeolite from waste kaolin. In order to simplify creation of the composites, the authors opted for a combination of glycerol and arabic gum as the plasticizer. Several films with different concentrations of the aforementioned types of biocarbon were produced, characterized (by optical microscopy, FTIR analysis and differential scanning calorimetry, as well as in terms of mechanical properties, water solubility, water uptake) and compared. An investigation was also made as to the effect of the given fillers on the growth of *Sinapis alba* in a practical test, as well as the biodegradability of the materials.

Experimental

Materials and chemicals

The following materials were used to prepare the polymeric films: polyvinylpyrrolidone (PVP, 10 kDa) was purchased from Alchimica with the purity of 98%; glycerol was supplied by Penta; and arabic gum was supplied by Lachema a.s. The filler comprised biocarbon and the synthetic zeolite; their basic characteristics are shown in **Table 1**.

The biocarbon took the form of dried or pyrolyzed cow manure. The dried biocarbon (DC) was prepared thus: raw cow manure was dried to remove all moisture under laboratory conditions until constant weight was achieved; it was ground and passed through a sieve (mesh size 0.1 X 0.1 mm). The pyrolyzed biocarbon—biochar (BCh) was obtained from raw cow manure by slow pyrolysis at a moderate temperature (JZD Fryšták, Czech Republic). Prior to the said matter being employed as a filler, it was ground in a Retsch MM301 Mixer Mill (Germany).

Table 1 Basic characteristics of the fillers (n = 3, average \pm standard deviation)

Filler	Elementary analysis				Particle size (μm)	Water adsorption (%)	pH _w
	C (%)	N (%)	H (%)	S (%)			
Z	–	–	–	–	1–50	0.86 \pm 0.02	10.11
DC	41.27 \pm 0.32	2.95 \pm 0.12	5.87 \pm 0.19	1.85 \pm 0.07	–	1.91 \pm 0.16	6.98
BCh	48.46 \pm 0.44	2.11 \pm 0.04	1.12 \pm 0.04	<ND*	1–50	3.03 \pm 0.19	10.40

*Below the limit of detection

The synthetic zeolite was kindly supplied by J. Kattauer (Faculty of Technology, UTB Zlin, Czech Republic). The synthetic zeolite was prepared in the laboratory from waste material containing kaolin produced by Sklopisek Strelec a.s. (Czech Republic). X-ray diffraction analysis (XRD) showed the presence of a zeolite P1 structure. Prior to being applied as a filler, the synthetic zeolite was ground in the Retsch MM301 Mixer Mill (Germany).

The remaining chemicals employed herein were of analytical purity and produced or delivered by Pliva-Lachema Brno (Czech Republic).

Characterization of the filler

Qualitative X-ray fluorescence analysis (XRF) was conducted on an ElvaX SER-01 (Elvatech Ltd., Ukraine) unit fitted with a silver X-ray lamp. Measurement was taken at current $I = 64 \mu\text{A}$ and the anode voltage of 10 kV, while the exposure time of the sample was 100 s. The samples were placed in special polyethylene attachments equipped with polypropylene foil.

Elemental analysis of CHNS was performed on an Automatic Elementar Analyzer (Thermo Fisher Scientific Inc.), involving a sample of 2-3 mg weighed at micro-analytical level to the precision of six decimal places.

The values for pH_w of the fillers were measured in demineralized water; the values for pH_w of the 4% w fillers water suspension were measured after 24 h stirring (100 rpm).

Preparation of the polymeric films based on PVP

The films were prepared by the casting method (**Fig. 1**). Firstly, a 10 wt% solution of PVP in water was made ready by stirring in a water bath (80 °C) until the PVP had completely dissolved. After such dissolution, 17 wt% of glycerol (GLY) was added. Meanwhile, in a parallel beaker, arabic gum (AG) (1 wt% to PVP) was dissolved in 5 ml of demineralized water and then the synthetic zeolite (2.5 wt% to PVP), and the appropriate amount of the processed biocarbon (0, 0.5, 1, 5 wt% to PVP) was added to the arabic gum solution. Finally, the contents of both beakers were mixed together and thoroughly homogenized, upon which this suspension was poured into a silicone form (12 x 7 cm).

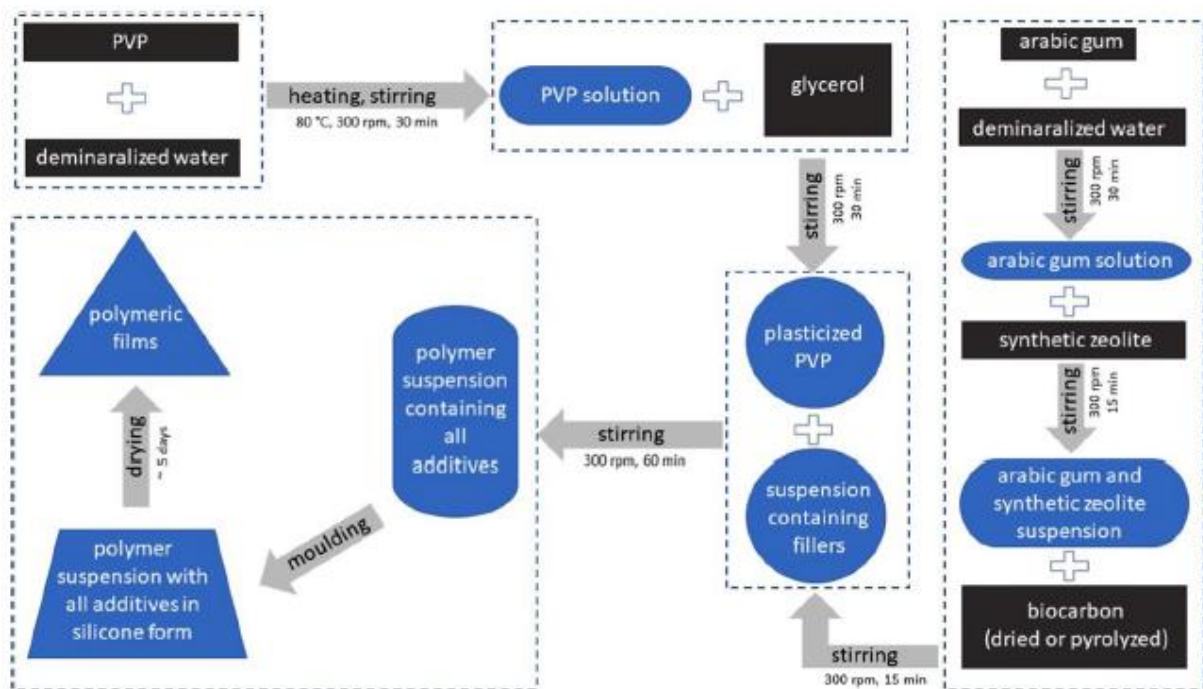


Fig. 1 Schematic illustration of the method used for the preparation of the polymeric films

The resultant cast films were dried in open-air conditions at $24.1 \pm 0.7 \text{ }^\circ\text{C}$ and a relative humidity of $23.6 \pm 0.8\%$ to let the solvent evaporate. A series with a specific amount of each type of the processed biocarbon was produced, and samples are summarized in **Table 2**.

Attenuated total reflectance infrared spectroscopy

FTIR spectra for all the films were recorded on a FTIR Nicolet iS10 unit (Thermo Scientific, USA), fitted with an ATR Smart MIRacle™ adapter containing a diamond crystal. Such analysis comprised 32 scans, at wave numbers ranging from 4000 to 500 cm⁻¹ and a spectral resolution of 4 cm⁻¹. The data gathered were evaluated in Omnic 8 software (Thermo Scientific, USA).









Scanning electron microscopy

The morphology of the fillers was studied on a scanning electron microscope (a Phenom Pro X device equipped with the Pro Suite; Phenom-World BV, Eindhoven, Netherlands). Images were taken at the magnification of 1000 x and 1050x. The unit was set to the acceleration voltage of 15 kV.

Film characterization with optical microscopy

This occurred with the films fixed to polystyrene Petri dishes (3.4 cm in diameter; TPP Techno Plastic Products AG) under an optical microscope (Nikon Eclipse 50i; Nikon, Japan). The surface distribution of the filler was revealed by the light transmitted.

Table 2 Sample codes, the composition of the prepared polymeric films in wt%, the thickness and the colours of the films

Sample code*	PVP	Plasticizers		Synthetic zeolite	Biocarbon	Th** (µm)	Colour of the film
		Glycerol	Arabic gum				
PVP	100	–	–	–	–	201 ± 06	
PVP/p	82	17	1	–	–	206 ± 14	
PVP/p/Z	79.5	17	1	2.5	–	257 ± 07	
<i>Dried</i>							
PVP/p/Z+0.5DC	79	17	1	2.5	0.5	222 ± 14	
PVP/p/Z+1DC	78.5	17	1	2.5	1.0	228 ± 28	
PVP/p/Z+5DC	74.5	17	1	2.5	5.0	324 ± 03	
<i>Pyrolyzed</i>							
PVP/p/Z+0.5BCh	79	17	1	2.5	0.5	213 ± 16	
PVP/p/Z+1BCh	78.5	17	1	2.5	1.0	204 ± 12	
PVP/p/Z+5BCh	74.5	17	1	2.5	5.0	209 ± 10	

*p—plasticizers, Z—synthetic zeolite, DC—dried biocarbon, BCh— pyrolyzed biocarbon (biochar)

**Thickness of films (n = 3, average ± standard deviation)

The fractured surfaces were imaged via polarized reflected light. Creation of the scale bar and analysis of filler coverage were carried out in ImageJ software, version 1.5 (W. Rasband, National Institutes of Health, USA). Marking of the entire surface covering was conducted manually with the “Threshold”

tool, and the relevant value(s) in per cent was obtained with the “Analyse particles” function for the displayed area.

Mechanical properties

The prepared films were assessed on a universal testing machine (Instron 3345; USA) with Bluehill 3 software at a crosshead speed of 10 mm·min⁻¹. A minimum of five dumb-bell-shaped specimens of dimensions 15 x 5 x 0.2 mm were tested for each type of film, and the results were averaged. All the samples were kept under conditions of 45% relative humidity at 25 °C beforehand.

Differential scanning calorimetry

Differential scanning calorimetry (DSC) was conducted on a Mettler Toledo DSC 1 unit (India). The samples were placed in aluminium cells (ca 10 mg), and scanning took place at the heating rate of 10 °C/min. and heating range of ambient to 210 °C. Prior to commencing this procedure, all the samples were stored in a desiccator at 25 °C. The glass transition temperature (T_g) for every sample was determined from the second heating scan. The melting point (T_m) of the polymeric films was evaluated from the first heating cycle.

Water solubility

The dried films were cut into square pieces of dimensions 5 x 5 x 0.2 mm and added into Erlenmeyer flasks with the appropriate amount of demineralized water. At a designated time, an aqueous phase sample was taken by a pipette and tested to determine the concentration of the solution, which involved determining its chemical oxygen demand (COD) in a closed system, in accordance with the international standard colorimetric method ISO 15,705:2002 [40, 41]. The water solubility (%) was calculated by Eq. (1).

$$\text{Water solubility} = \frac{\text{COD}_0 - \text{COD}_n}{\text{COD}_0} \cdot 100 \quad (1)$$

where COD₀ represents the COD of the dried films at the beginning of the test and COD_n is the COD measured at an appropriate interval (n).

The courses over time (WS = f(t)) for water solubility (WS) of the pure PVP or prepared films were described by regression, applying Eq. (2) for first-order substrate kinetics [42].

$$\text{WS} = \text{WS}_\infty \cdot (1 - \exp^{-k \cdot t}) \quad (2)$$

where WS_∞ is the regression coefficient representing the limit value in infinite time (%), k is the constant rate (min⁻¹) and t is the time (min).

Water uptake

The water uptake of the pre-dried polymeric films was gauged in a humidity chamber with ca 54% relative humidity (RH), with subsequent gravimetric analysis. The difference in weight was measured at specified intervals until no change in weight (± 0.001 g) was observed. The extent of water uptake in per cent was calculated afterwards, according to Eq. (3):

$$\text{Water uptake} = \frac{w_0 - w_n}{w_n} \cdot 100 \quad (3)$$

where w_0 is the weight of the dried films at the beginning of the experiment and w_n is the weight at a given interval (n).

Biodegradability of the polymeric films in the soil environment

This aspect was investigated on an OxiTop®Control respirometric device (WTW GmbH, Germany) for 30 days at 25 °C. To this end, 50 ± 0.1 g of agricultural soil (sourced in Zlin, Czech Republic) was added into 0.25-l respirometric bottles and supplemented with approximately 80 mg of the test sample. The soil tests were performed at 25 ± 1 °C, and all measurements were taken in triplicate. Determinations were performed at the beginning and end of each test, these pertaining to the dry matter of soil and the value for soil exchange capacity (pHKCl) for the purpose of checking on the process. At the end of the test, moisture equalled approximately 55% and pH_{KCl} about 7.2. The percentage of biodegradation was evaluated by Eq. (4):

$$\text{Biodegradation} = \frac{(\text{BOD}_{\text{sample}} - \text{BOD}_{\text{blank}})/w_{\text{sample}}}{\text{COD}} \cdot 100 \quad (4)$$

where BOD_{BLANK} represents the biological oxygen demand (mg) of the blank (the endogenous respiration of the soil microorganisms), BOD_{SAMPLE} represents the biological oxygen demand (mg) of the sample during biodegradation of the tested polymeric films, COD is the experimental determination of chemical oxygen demand (mg g⁻¹) [40] of the polymeric film and w is the weight of the tested polymeric material (g).

So as to assess whether biodegradation proceeded in accordance with the rule of additivity, i.e. the final point of biodegradation at the given time—denoted by the sum of biodegradation values for particular components, or if physico-chemical and microbial reactions (positive or negative) occurred in the system, Eq. (5) was applied [43]:

$$\text{Additivity} = w_1 \times D_1 + w_2 \times D_2 + \dots \dots \dots + w_n \times D_n \quad (5)$$

where values D_1 - D_n are calculated in accordance with the equation for pure components (4) and values w_1 - w_n represent the mass fractions of particular components in the polymeric films (Table 2).

Screening plant growth test (*Sinapis alba*)

Certified seeds of *Sinapis alba* were purchased from the Semo Company (Semo a.s., Czech Republic). Preliminary incubation revealed that all the seeds utilized in this study showed a rate of germination exceeding 90%.

The screening plant growth test [44] was performed in 40-ml polystyrene cultivation vessels filled with a mixture of natural soil and perlite in a 3:1 ratio. Seed encapsulation was created on the basis of the polymeric films with 5 wt% of fillers, whereby the films were attached to each other to ensure placement of a *Sinapis alba* seed between them. The resultant tapes were cut into small 1 x 1 cm squares so that each square contained a seed in the middle. These squares were placed in the soil to a depth of about 0.5 cm below the surface. The cultivation vessels were placed in a thermostat at 25 ± 1 °C with continuous illumination of 7000 lx and 55% RH on a 1-cm-high plastic mat to allow for drainage and prevent the cultivation vessels from taking up any release of moisture from the surrounding cultivation vessels. This experiment was run for 12 days, and the seeds were regularly watered [44]. No fertilizers were added during the experiment.

After cessation of the experiment, values were gauged for the mean lengths of the shoots, roots and total wet biomass. The elongation of the main shoot of the plant was measured every day.

The relative growth rate of each plant (RGR) was evaluated by two parameters (PP) according to Eq. (6). During cultivation, the height of the whole plant was measured at 24-h intervals and this was then applied to calculate the relative growth rate of germination (RGR_{ger}). The growth rate of the plants was worked out at the close of the test on the basis of fresh mass (RGR_{FW}) [45].

$$\text{RGR} = \frac{\ln(\text{PP}_j) - \ln(\text{PP}_i)}{t_j - t_i} \quad (6)$$

where RGR is the relative growth rate from time i to j , PP_i and PP_j are the endpoint (fresh mass or plant height) in the test or control vessel at time i and j , respectively, and t is the time period from i to j [45].

The extent of accumulation of elements transferred from the fillers into the plant was determined on an atomic absorption spectrometer (AAS; Analytik Jena AG—contrAA 300). Prior to analysis, the plant samples were carefully cleaned and rinsed once with tap water, once with distilled water and finally twice with ultra-pure water to remove any residual trace of the polymeric films. All the samples were dried separately for 24 h at 80 °C. The plant samples (ca 0.2 g) were mineralized in 2.5 ml nitric acid and 0.5 ml peroxide for 21 min in a MLS 1200 mega microwave system (Milestone s. r. l., Sorisole, Italy).

Results and discussion

The research presented herein was concerned with preparing and characterizing polymeric films based on polyvinylpyrrolidone (PVP) as the matrix, while the following substances were utilized as fillers: synthetic zeolite fabricated from waste kaolin and biocarbon in dried or pyrolyzed form. The polymeric films were prepared with the aim of potential usage in agro-chemistry. According to Raya-Moreno et al. [25] and Uzoma et al. [26], the release of elements from biocarbon could have a potential positive effect on the soil environment.

Visual observation of the polymeric films obtained by casting method showed that all samples had good elastic properties and did not burst. Biocarbon particles incorporation led to a significant change in the colour of the polymeric films from a yellow-brown colour to a variety of grey and black depending on the filler type and concentration (**Table 2**). The polymeric films filled with synthetic zeolite were pale yellow in colour. The polymeric films filled with synthetic zeolite and DC were light brown to dark brown, and films filled with synthetic zeolite and BCh were grey to black in colour.

Estimation of the nature of the interactions

FTIR spectroscopy is a very powerful technique to detect the intermolecular interactions between polymer, plasticizer and fillers. In the prepared polymeric films, it is expected that intermolecular hydrogen bonding between the PVP and the plasticizers [5] and the hydrogen bond between PVP and zeolite [46] might be created. The intermolecular interaction through hydrogen bonding can be characterized, especially by FTIR, because the specific interaction affects the local electron density and the corresponding frequency shift can be observed [47].

To gain a deeper understanding of these interactions, the FTIR spectra of all the prepared polymeric films were studied. **Figure 2** details the IR spectra of the prepared films.

To gain a deeper understanding of these interactions, the FTIR spectra of all the prepared polymeric films were studied. **Figure 2** details the IR spectra of the prepared films.

The FTIR spectrum for pure PVP (**Fig. 2**, spectrum B) contains characteristic chemical bonds. The strong absorption band at 1666 cm^{-1} represents the carbonyl group ($\text{C}=\text{O}$) from the pyrrolidone ring of the polymer. Another peak at 1286 cm^{-1} is due to the presence of C-N stretching. The absorption bands at 1493 , 1469 and 1426 cm^{-1} denote the vibration of the pyrrolidone ring, while the two bands located at 2951 and 2886 cm^{-1} pertain to the asymmetrical and symmetrical stretching of $-\text{CH}_2$ groups and vibration of the aliphatic compound $-\text{CH}_2$, respectively.

Regarding the plasticized PVP sample, the broad absorption band observed in the wavenumber range of $3600\text{--}3000\text{ cm}^{-1}$ splits into two distinct bands. Since PVP is a hydrophilic polymer, it has a tendency to adsorb water molecules. Therefore, the appearance of two distinct bands at 3380 cm^{-1} and 3290 cm^{-1} suggests different states of adsorbed water in the system. Nesić et al. [5] proposed that the lowest wavenumber for the OH stretching band related to water molecules strongly bound to the given polymers, whereas OH groups at high frequencies were associated with free water. Herein, the intensity of these two bands is seen to significantly increase with the addition of glycerol, as a result of the greater amount of hydroxyl groups in the system. Two significant peaks also appear at around 1111 cm^{-1} and 1046 cm^{-1} , stemming from such supplementation of glycerol (**Fig. 2a**). The shoulder-like peak at 1046 cm^{-1} is an expression of the overlapping stretching vibrations of the C-O linkage in C1 and C3 from glycerol and the C-C stretching of the pyrrolidone ring from the PVP, while the peak at 1070 cm^{-1} is related to the overlapping stretching vibrations of the C-O and C-N groups from glycerol and PVP, respectively, in agreement with Nesić et al. [5]. A shift from 1666 to 1650 cm^{-1} is visible for the peak characterizing the $\text{C}=\text{O}$ group in the pyrrolidone ring of the PVP; this suggests that interactions had taken place in the form of hydrogen bonds between the carbonyl group in the pyrrolidone ring and the plasticizers, i.e. the $-\text{OH}$ groups.

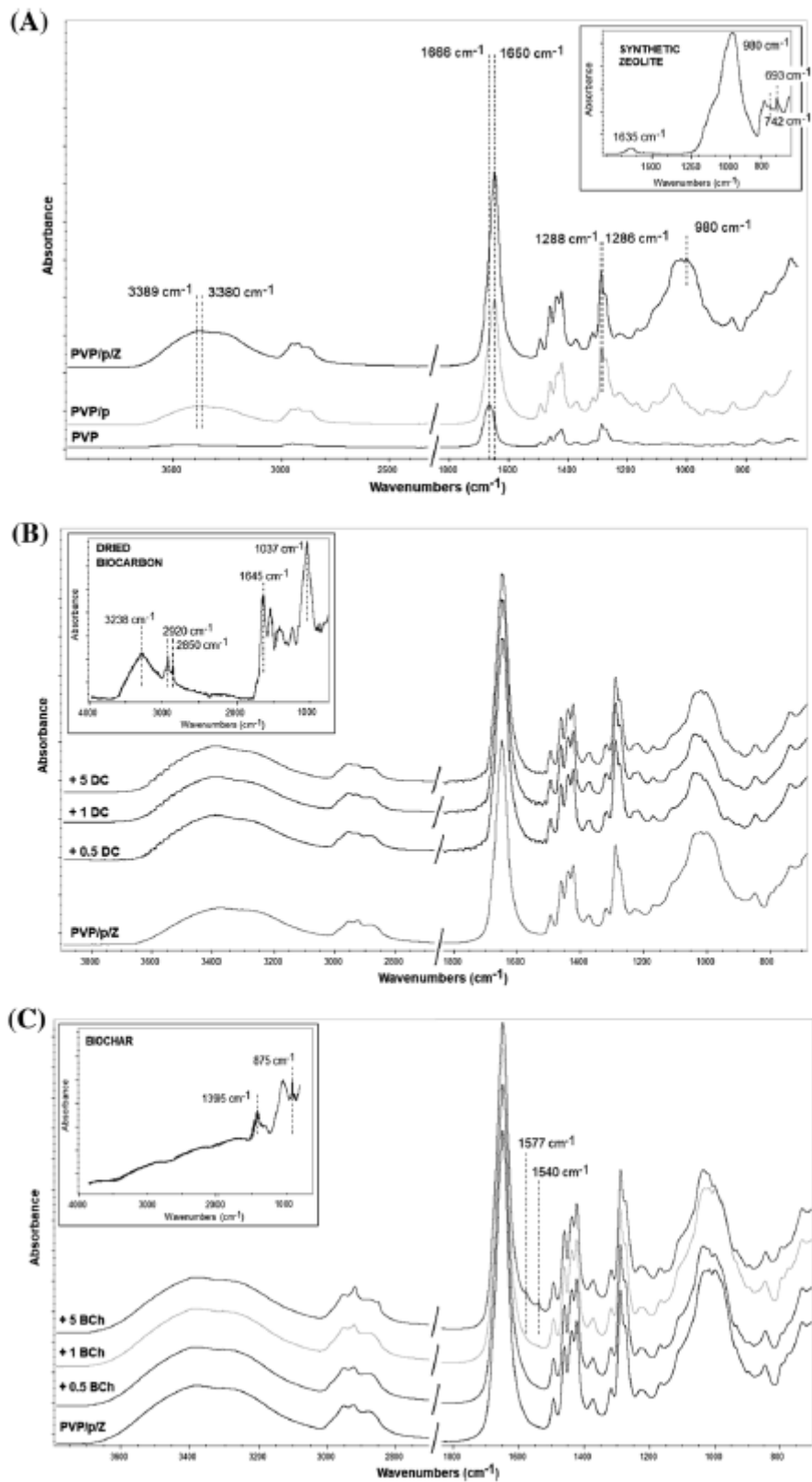


Fig. 2 FTIR spectra for the prepared polymeric films: **a** PVP, plasticized PVP (PVP/p) and plasticized PVP/synthetic zeolite (PVP/p/Z); **b** PVP/dried biocarbon (PVP/p/Z + DC); and **c** PVP/biochar (PVP/p/Z + BCh)

According to Liu et al. [48], for the zeolite P1, the bands at around 1635 cm^{-1} and 3382 cm^{-1} belong to the vibrations of hydroxyl groups or the solid-phase hydrate of water in the zeolite channels. The broad peak at 3382 cm^{-1} indicates the stretching vibration of hydroxyl, and the peak at 1635 cm^{-1} represents H-O-H bending vibration. The band at 980 cm^{-1} denotes the asymmetrical stretching vibration of TO_4 (T = Si or Al) tetrahedral. Those at 742 and 693 cm^{-1} for the zeolite P1 are attributed to the symmetrical stretching vibration of the internal tetrahedron, while that visible at 605 cm^{-1} corresponds to the presence of a double ring in the zeolite P1 framework.

Shifting the IR bands of the outer -OH groups of the blends PVP/p/Z to a lower frequency (from 3389 cm^{-1} to 3380 cm^{-1}) revealed that certain -OH groups were involved in hydrogen bonding with the carbonyl group or with the N atom of the PVP. In addition to these band-related assignments, the conjugation of a lone pair of N with C = O increased the stretching vibration of the C-N single bond, which had the effect of raising the stretching frequency for the C-N bond from 1286 to 1288 cm^{-1} . It was assumed that, due to the affinity of PVP with solvent water molecules, it readily diffused inside the porous structure of the synthetic zeolite [46].

According to Cantrell et al. [49], the broad band for the DC close to 3282 cm^{-1} is attributable to the stretching vibration of hydrogen-bonded hydroxyl groups. The asymmetrical (2920 cm^{-1}) and symmetrical (2850 cm^{-1}) C-H stretching bands are associated with aliphatic functional groups in the biopolymers. In addition to these band assignments, C = O stretching vibrations for amides are denoted at 1645 cm^{-1} . The absorption band for amide in this region is likely to have resulted from the carbonyl stretching vibration of the peptide bond, rather than the N-H bending and C-N stretching at lower wave values. Amides are often assigned in the FTIR analysis of dried biocarbon as the protein-specific band, as opposed to primary amines. Additional inorganic components such as sulphates and silicates could also have contributed to the broad and intensive peak at 940-1200 cm^{-1} . The pinnacle of this region at band 1037 cm^{-1} is attributed to the symmetrical C-O stretching for cellulose, hemicellulose and lignin, which are sometimes found in bedding material and partially digested feed. Two noticeable peaks at 1236 cm^{-1} and 1160 cm^{-1} are typical for the DC, the former at 1236 cm^{-1} pertaining to C-H stretching and OH deformation of COOH along with C-O stretching of aryl esters, while the latter at 1160 cm^{-1} signifies an asymmetrical C-O stretching characteristic of C-O-C in cellulose and hemicelluloses. Aromatic C = C stretching (1450-1379 cm^{-1}) and out-of-plane deformation by aromatic C-H groups (875 cm^{-1}) are also observable; see also Cantrell et al. [49].

For the biochar, most of the spectral features of the DC, except for the region of 1600-700 cm^{-1} , went undetected and the spectrum resembled pure graphite. (i) The spectral range of 1600-700 cm^{-1} was identified with increased aromatic C=C stretching (1395 cm^{-1}) and out-of-plane deformation by aromatic C-H groups (875 cm^{-1}), probably as a consequence of transformation products of lignin and cellulose; (ii) but a minor peak at 1581 cm^{-1} was assigned to C = C and C=N functional groups; and (iii) the peak close to 1420 cm^{-1} could have arisen from calcite and other carbonate mineral components (CO_3^{2-}) of the manure-originating biochar; see also Cantrell et al. [49]. Differences between the infrared spectra for the DC and BCh reflect the water loss, combustion of organic matter and concentration of mineral components brought about by heat-induced loss of mass.

The FTIR spectra for the polymeric films/biocarbon (Fig. 2b and c) highlight that little or no obvious variation exists between the locations of the IR absorption peaks for the PVP/p/Z + DC and PVP/p/Z + BCh blends with respect to PVP/p/Z. Minor peaks are only visible for PVP/p/Z + 5BCh between 1577 cm^{-1} and 1540 cm^{-1} , linked with NH valence vibrations from the nitrogen components of the biochar. No detection occurred of the appearance of new bands or significant shift in the spectra for the blends, although the corresponding peak intensities changed in accordance with blend composition to some

extent. These results show that the biocarbon (DC or BCh) had an additive effect on the final chemical disposition of the blends.

Mechanical properties

Incorporating particulate fillers has the capacity to modify the mechanical properties of polymers in numerous ways, depending on the given particle size, loading, particle-matrix interfacial adhesion and microstructure of the composites. The maximum strength that can be sustained by microparticle composites under uniaxial tensile loading depends on the effective stress transfer between the matrix and filler particles [50].

In order to obtain further data on such mechanical properties, the authors decided to carry out tensile tests. The subsequent evaluated values for Young's modulus (MPa) and elongation at break (%) are given in Fig. 3. Since the pure PVP film proved too brittle, it was not possible to discern its mechanical properties thoroughly. Hence, a sample of PVP/p with plasticizer content was applied as a reference material to observe the effect of the fillers.

Figure 3 shows that the presence of synthetic zeolite moderately increases the Young's modulus of the composites, as also observed by Mahmoudi Beram et al. [51]; thus, said zeolites have the potential to enhance the mechanical properties of polymeric films. This 12% increase probably arises through interactions between the PVP and synthetic zeolite (see the FTIR analysis).

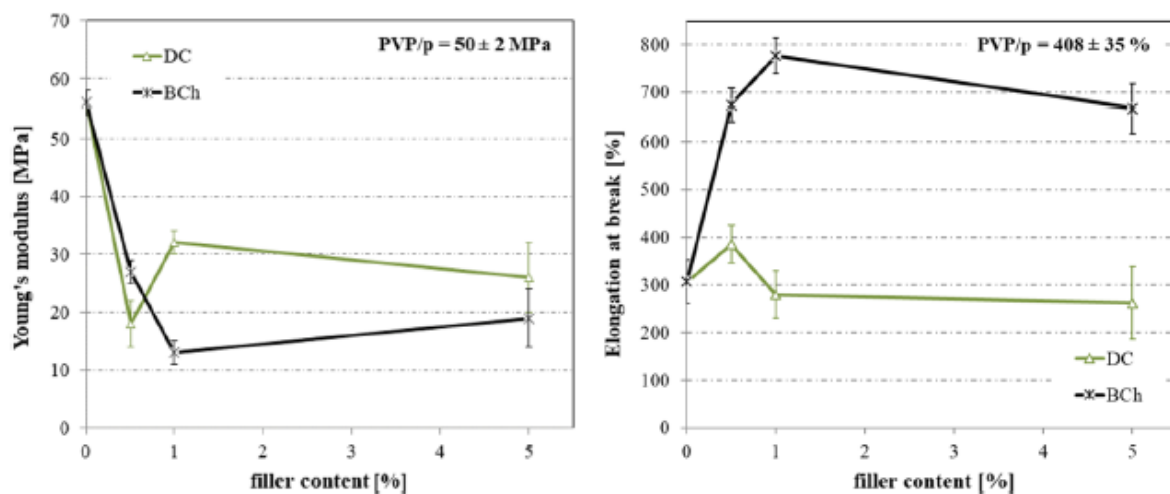


Fig. 3 Variation in Young's modulus (left) and elongation at break (right) with filler content (n = 5, average ± standard deviation)

However, significant alteration was seen for the DCs and BChs in comparison with PVP/p or PVP/p/Z. The general consensus was that utilizing the biocarbon in the PVP matrix reduced values for Young's modulus. Such a decrease in Young's modulus by up to 67% was evident for materials filled with the DCs, this reaching 76% for those filled with the BChs. A similar trend was witnessed in values for elongation at break for the polymeric films with the DC filler. Raising the content of DC instigated poor interfacial bonding of heterogeneous particles with the PVP matrix (Fig. 8, optical microscopy), thereby diminishing the elastic property of the polymeric films. In contrast, results for elongation at break for the BCh-filled films constituted far more interesting findings, where such values were double those of

PVP/p and PVP/p/Z, indicating the greater flexibility of PVP/p/Z + BCh. This was unusual since the majority of biochar-filled composites usually turn brittle upon addition of even small amounts of biochar [22-24]. In this context, the authors concluded that the layers of graphite in the biochar were able to inhibit or at least to slow down the propagation of cracks by deviating them from their normal pattern of tear.

Differential scanning calorimetry

DSC analysis was performed to determine the characteristic temperatures of the prepared polymeric films, and the results of this analysis went towards assessing whether the particles of synthetic zeolite/biochar acted as potential nucleation sites, from which the growth of crystals could be initiated in the PVP matrix. This aspect had the potential to exert a major impact on the biodegradability of materials in a biotic environment, as the amorphous portions of the polymer chains are generally more susceptible to hydrolysis and biodegradation than some crystalline parts of polymers. In the case of the DC filler, any nucleation effect of the particles was not expected, since this type of filler predominantly contains amorphous cellulose compounds.

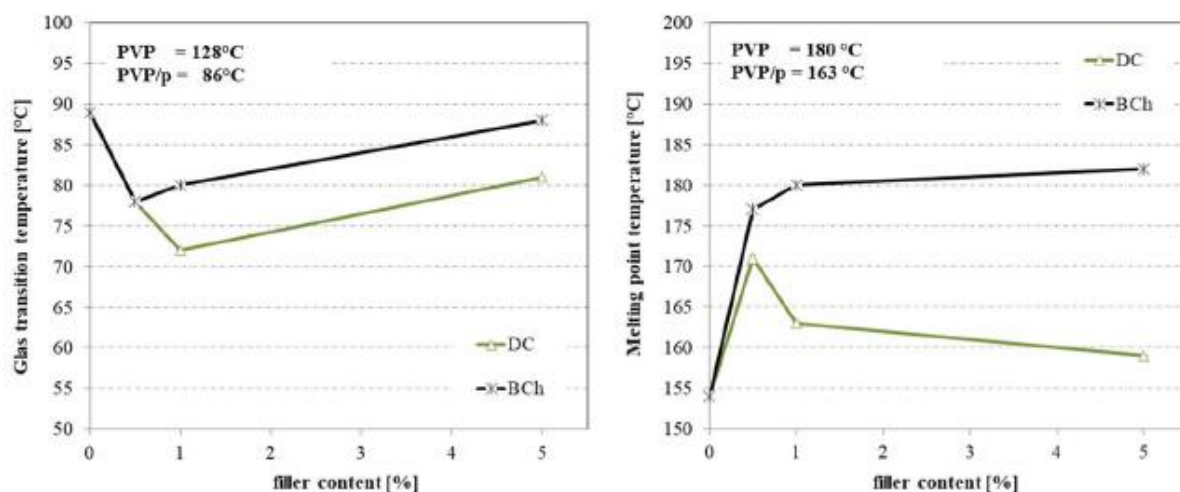


Fig. 4 Variation in glass transition temperature (left) and melting point temperature (right) with dependence on filler content (n = 5, average \pm standard deviation)

Evaluating the glass transition temperature and melting temperature via DSC waveforms obtained through measurements (Fig. 4) demonstrated that the presence of both plasticizers (glycerol and arabic gum) and fillers exerted an effect on the thermal properties of the prepared polymeric films.

It should be emphasized that PVP is known to be predominantly amorphous; hence, the corresponding T_m peak at 180 °C was small (DSC curves are not presented herein) [52, 53]. As expected, PVP displayed a T_g close to 128 °C, which was high because of the presence of the rigid pyrrolidone groups.

Adding a plasticizer brings about microstructural changes in a polymer matrix through reduction occurring in intermolecular forces between the polymer chains, which is why diminished T_g values were expected. This was confirmed, since supplementation with glycerol and arabic gum as plasticizers

caused a drop in the value for T_g by 42 °C, attributable to the emergence of the hydrogen-bonded network observed by FTIR spectroscopy. It was seen that T_m decreased from 180 to 163 °C.

It was further established that adding synthetic zeolite to the PVP/p mixture triggered a slight increase (by 3 °C) in T_g to 89 °C and a drop in T_m by up to ca 10 °C, suggesting no crystalline phase was formed by such supplementation with the zeolite particles.

As regards the addition of other fillers, the presence of DC at 0.5% w/w increased the T_m of the polymeric films, in comparison with PVP/p/Z, to 171 °C. As the concentration of the filler was raised, this value gradually decreased, e.g. the sample of PVP/p/Z + 5DC demonstrated a T_m of 159 °C. Due to the content of DC, T_g was observed to drop. In the case of the PVP/p/Z + 1DC sample, it fell to 72 °C; however, no trend was discernible as a result of increasing the concentration of the filler. This variability in T_g values might have been due to the heterogeneous nature of the natural, untreated DC filler.

For samples containing BCh, the T_m measured was relatively high compared to the DC, ranging between 177 °C and 182 °C based on the filler. This suggested that the BCh particles with a relatively large surface area improved the thermal stability of the PVP when dispersed in it. By adding 0.5% of BCh, T_g decreased by ca 10 °C compared to PVP/p/Z. However, as the percentage of BCh went up, T_g increased to a level comparable to PVP/p/Z.

Water solubility and water uptake

The following experiments were conducted to investigate water solubility and water uptake. The results from these analyses are given in **Fig. 5**.

Water uptake affects mechanical properties and chemical stability. Together with biodegradability, it is one of the most important properties for practical applications and subsequent usage of biodegradable polymeric films. Since the prepared films were proposed as the carriers of seeds for sowing purposes, some extent of hygroscopicity of the film might be an advantage, e.g. when microorganisms are employed to aid plant growth [54, 55].

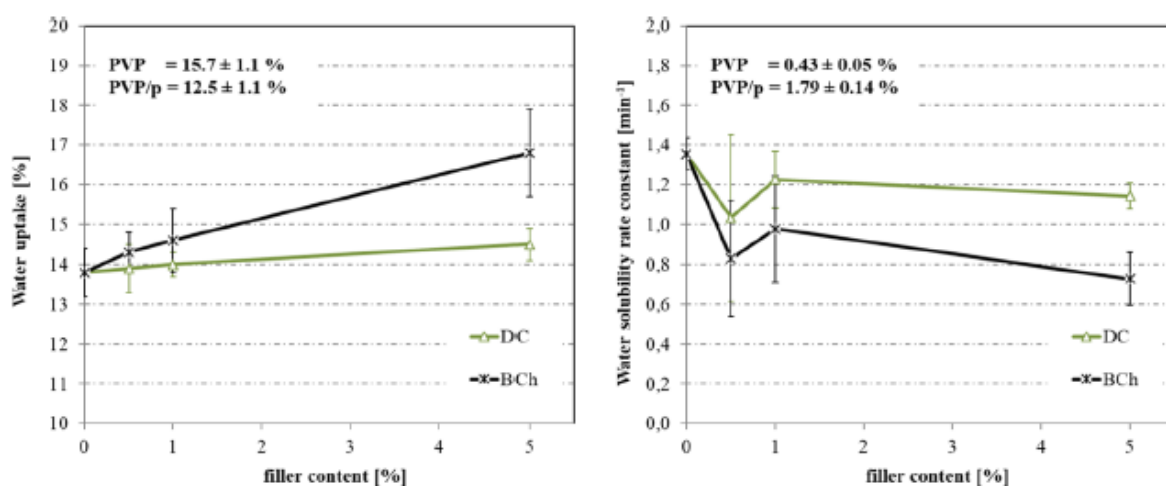


Fig. 5 Water uptake at 54% RH of the films as a function of filler content after 10 days (at equilibrium), and the rate of water solubility (constant) as a function of filler content; the DC films had been loaded with the dried biocarbon, and the BCh films with biochar (n = 3, average ± standard deviation)

PVP is a hydrophilic polymer with a great capacity for water adsorption. An experiment was conducted to determine water uptake at the relative humidity of 54% (a potential application of the polymeric films in the soil environment). The pure PVP demonstrated $15.7 \pm 1.1\%$ as its value for water uptake, whereas adding glycerol and arabic gum as plasticizers brought about a slight decrease to $12.5 \pm 1.1\%$. This 3% drop could have been caused by the formation of hydrogen bonds between the carbonyl group in the pyrrolidone ring and the -OH plasticizers (**Fig. 2**). The presence of synthetic zeolite in the film (PVP/p/Z) slightly suppressed this negative effect, and the value for water uptake was close to those specified for pure PVP, i.e. $13.8 \pm 0.5\%$, due to the hygroscopicity of the synthetic zeolite.

Yusefi et al. [35] stated that the natural fibres were also both hydrophilic and hygroscopic in nature; therefore, higher levels of DC content had the ability to initiate greater water uptake. However, this phenomenon did not arise during the experiment presented herein. The water uptake values for the DC-filled films were at around 14% (PVP/p/Z + 0.5DC, $14.9 \pm 0.5\%$; PVP/p/Z + 1DC, $14.0 \pm 0.2\%$; PVP/p/Z + 5DC, $14.5 \pm 0.3\%$).

The highest value for water uptake was discerned for PVP/p/Z + 5BCh ($16.8 \pm 1.9\%$), probably due to the greater absorption of water by the biochar itself compared to other fillers. At lower concentrations of filler, though, this aspect was negligible (PVP/p/Z + 0.5BCh, $14.3 \pm 0.4\%$; PVP/p/Z + 1BCh, $14.6 \pm 0.7\%$).

Based on the findings obtained, it can be stated that the extent of water uptake was satisfactory for the proposed films in terms of handling and any further application.

High solubility is a desirable characteristic for biodegradable films because rise in solubility enhances the level of biodegradability. A highly soluble film is an advantage when utilized in an agricultural product. Therefore, study was made as to the influence of the individual fillers on the solubility of the polymeric films. All the samples were highly soluble in water (100% solubility, according to the COD results); hence, the dissolution profiles for them were evaluated by a mathematical model of order I [42]. The rates of dissolution for the polymeric films were expressed as the rate constant for water solubility in min^{-1} ; see **Fig. 5** for details.

The matrix and plasticizers proved well soluble. The presence of the glycerol and arabic gum heightened the solubility of the plasticized PVP film, exceeding the same for the pure PVP film. Adding the plasticizers (glycerol and arabic gum) increased the dissolution rate of the polymeric film by approximately four times in magnitude. This finding was expected, as glycerol is a substance easily soluble in water. The addition of the synthetic zeolite reduced the dissolution rate from $1.79 \text{ min}^{-1} \pm 0.14$ to $1.35 \pm 0.08 \text{ min}^{-1}$. Water solubility is related to the content of free hydroxyl groups in the polymeric matrix; thus, the reduction in the dissolution rate of the PVP/p/Z films may have been due to hydrogen bonding occurring between the PVP and synthetic zeolite (**Fig. 2**). An additional assumption was that the PVP had been gradually released from the porous structure of synthetic zeolite.

The polymeric films containing DC or BCh dissolved slightly slower than the PVP/p/Z film: 0.5DC $1.05 \pm 0.41 \text{ min}^{-1}$; 1DC $1.23 \pm 0.14 \text{ min}^{-1}$; 5DC $1.14 \pm 0.06 \text{ min}^{-1}$; 0.5BCh $0.83 \pm 0.29 \text{ min}^{-1}$; 1BCh $0.98 \pm 0.27 \text{ min}^{-1}$; and 5BCh $0.73 \pm 0.13 \text{ min}^{-1}$. However, the amount of the given filler (denoted in per cent) had no statistically significant effect on water solubility.

Biodegradability of the polymeric films in the soil environment

Biodegradation experiments were conducted to investigate the biological degradation of the prepared films and the impact of the fillers on the microbial decomposition of PVP in the soil environment. The results are detailed in **Fig. 6**.

As can be seen, $12.8 \pm 2\%$ was measured for biodegradation of the PVP/p polymer film, which approximately corresponded to decomposition of the plasticizers (glycerol and arabic gum) alone. However, the same material supplemented with the synthetic zeolite showed the potential for slightly more degradation, probably due to the positive effect of the zeolite, which contained macronutrients such as Fe, Mg and Mn (see XRF analysis), on the soil microorganisms.

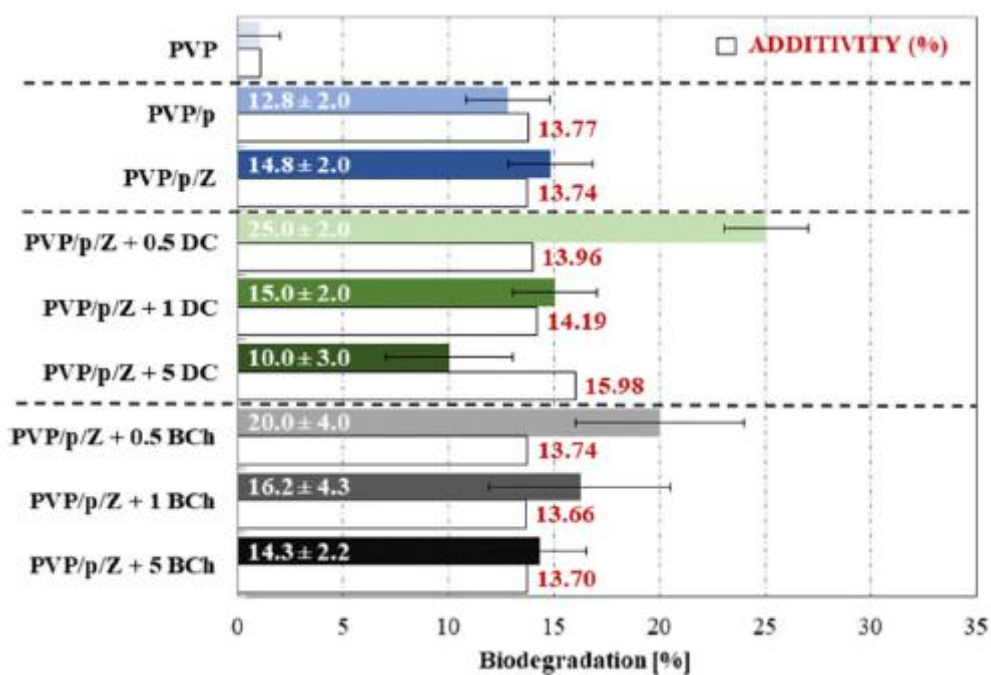


Fig. 6 Biodegradation of the polymeric films in the soil environment (n = 3, average \pm standard deviation)

The films containing DC and BCh demonstrated greater biodegradation (about twice the extent). The highest level of biodegradation was seen for the material containing 0.5% w/w DC: $25.0 \pm 2.0\%$. Comparing the actual measured values and the values calculated according to the additivity rule (the contribution of weight of the individual components to degradation—**Fig. 6**), revealed that the extent of biodegradation was ca. 10% higher. Therefore, decomposition could have occurred of the filler (DC) containing lignocellulose, with the potential for subsequent initiation of degradation of the polymeric matrix. However, when DC concentration was higher, the percentage of degradation decreased (PVP/p/Z + 5DC- $10.0 \pm 3.0\%$) and was almost equal to that for PVP/p.

It was not assumed that the samples with BCh had followed the same course of action as those containing lignocellulose, i.e. formation of an enzymatic apparatus through biodegradation of the filler. However, pyrolyzed biocarbon has the potential to become a source of macro- or micro-genic elements for the metabolisms of soil-based microorganisms, maybe in turn aiding their propagation and growth. These findings as to the degradation of the polymeric films on the basis of BCh in the soil environment lend support to the claim by Chen et al. [27] that the presence of a biochar could promote the biodegradation of polymeric films. Herein, findings on biodegradation of the polymeric films

supplemented with BCh in the soil environment showed that the highest extent of biodegradation was achieved for those films filled with 0.5% BCh w/w: $20.0 \pm 4.0\%$. During comparison of the actual measured values for biodegradation of the polymer films with BCh, a similar trend was observed in contrast to those containing the DC, albeit less significant. An increase in filler concentration brought about a parallel drop in the percentage of biodegradation.

The trend for decrease in the extent of biodegradation of the polymeric films alongside parallel rise in filler concentration might have been instigated by the following three causes: (i) it is reported that the water-soluble components of polymeric films can be adsorbed by particles of DC or BCh, although conducting a sorption experiment did not confirm this (data not presented); (ii) it is known that, in the biological degradation of polymers by microorganisms, amorphous fractions are preferred over crystalline fractions; thus, an assumption is that the BCh particles and those in the DC could have acted as nucleation agents, potentially leading to formation of a crystalline phase; (iii) PVP has complexation effects; hence complexes were likely to have formed between the PVP and BCh substances and in the DC, possibly resulting in slower biodegradation. It should be noted that such soil tests take a considerable time; therefore, longer testing periods would be needed to clarify the exact causes, with concurrent investigation of other characteristics of the materials, by means such as nuclear magnetic resonance spectroscopy and X-ray diffraction.

Examination of morphology

It is well known that the properties of polymer films greatly depend on morphological structure of the fillers. To gain a deeper understanding of the influence of the fillers morphology and their distribution in the polymeric films on the mechanical properties, the microscopic observation of the fillers and all the prepared polymeric films was carried out.

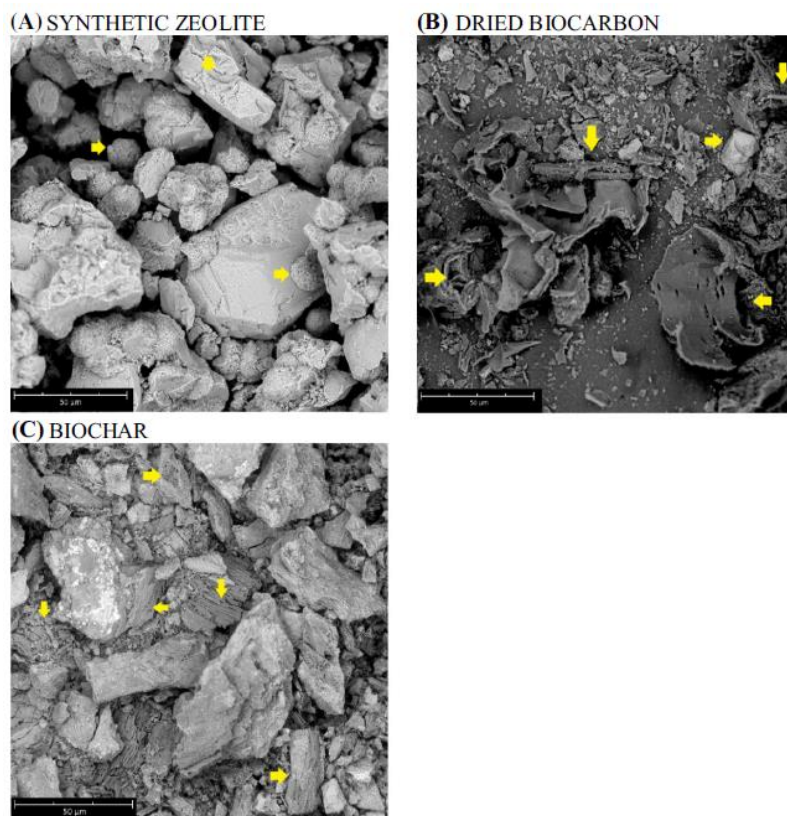


Fig. 7 SEM images of the fillers

Firstly was studied the morphology of synthetic zeolite and biocarbon particles by SEM (**Fig. 7**). The SEM images of the fillers (i.e. synthetic zeolite, dried biocarbon and biochar) show that a great difference existed between the given fillers. The porous structure of the fillers is clearly visible (**Fig. 7**), revealing the variation in shape of the macropores and mesopores. The images for the dried biocarbon (DC) filler plainly demonstrate that the particles consisted of a variety of morphologies (**Fig. 7**). It is clear that the porous particles varied in size, appearing to be conglomerations of spherules, flakes and asymmetrical particles. The other mineral form observed was rod- or needle-like, which occasionally gathered together as clusters. The SEM image in **Fig. 7** illustrates the surface texture and porosity of BCh, where holes and small openings are visible on the surface, thereby increasing the area of contact. The BCh particles were heterogeneous in shape, i.e. completely random without correlation between the particles, with pointed or sharp edges. The form of some BCh particles resembled the structure of the chopped plant fibres from which the biocarbon was pyrolyzed. Such aspects play a huge role in the mechanical properties of the blends, as discussed in this manuscript. As for the synthetic zeolite particles, their morphology took on a more homogeneous appearance than the DC and BCh samples, with a tendency for a globular like contour (decreased aspect ratio). Fracturing of the zeolite particles revealed their porous structure.

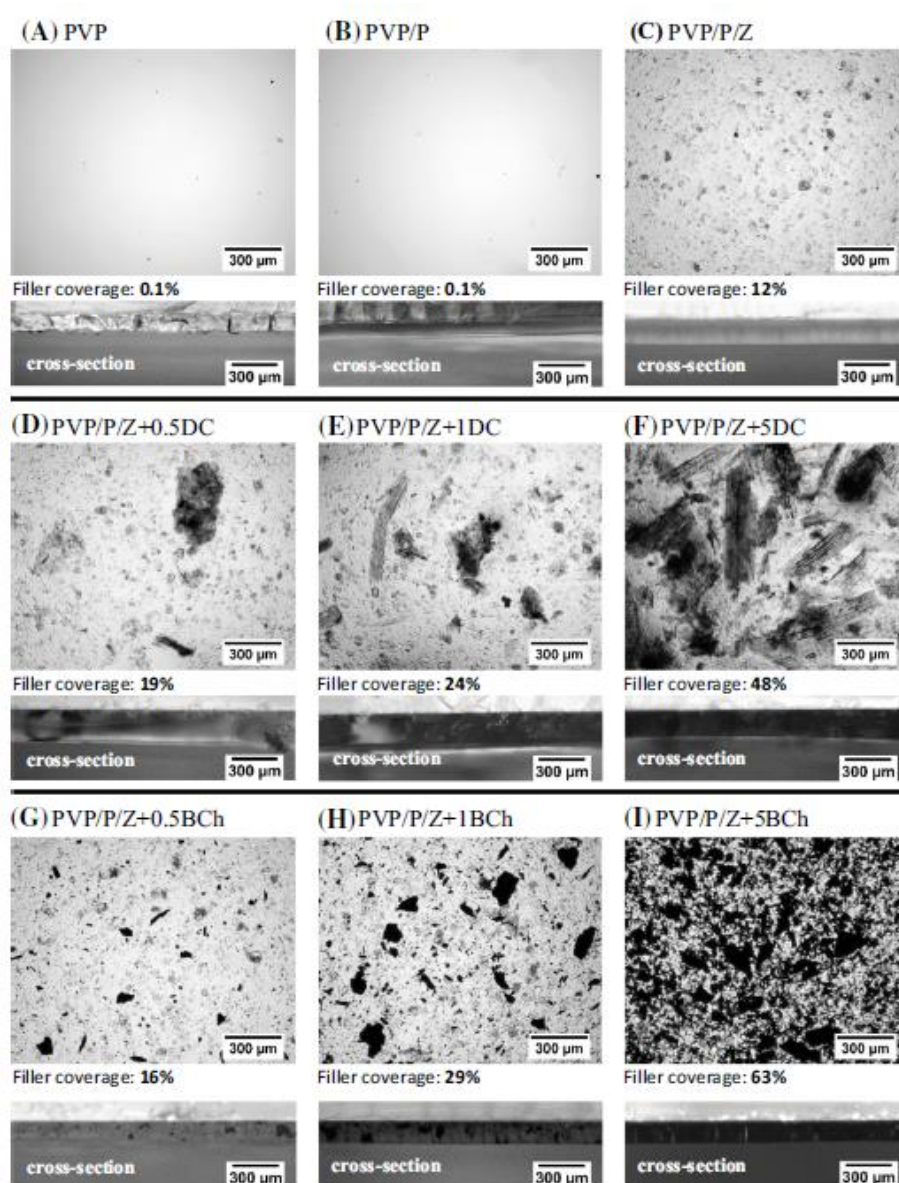


Fig. 8 Optical microscopy images of the polymeric films

Morphological characterization of the PVP films supplemented with the fillers took place via optical microscopy, since SEM-based image analysis did not provide enough relevant data. **Figure 8** shows optical micrographs for pure PVP, plasticized PVP and PVP samples that differed in the content of filler.

In line with expectations for the PVP and plasticized PVP films (**Fig. 8a** and **b**), no particles are evident in the surface area or cross section, except for minor impurities. The extent of coverage of the surface by the filler (particles of the same) is equivalent to 0.1% maximally.

In the PVP/p/Z sample (**Fig. 8c**), particles of zeolite are evident in both the surface area and the cross section. The extent of surface coverage for the zeolite particles is equal to 12%. Zeolite particles are uniformly distributed throughout the matrix, as visible in the optical micrographs of the cross sections.

The optical micrographs for PVP/p/Z + DC (**Fig. 8d-f**) show nonhomogeneous distribution of the DC particles (some voids exist), which acted as weak or stress concentration points during mechanical testing. Young's modulus (MPa) and elongation at break (%) in relation to defects (micropores in the biocarbon particle) are discussed in the section on mechanical properties. In accordance with the SEM analysis of the filler, particles of conglomerations of spherules, flakes, rod- or needlelike clusters and asymmetrical particles were discerned in the films with DC. The comparison made in these figures reveals that, in proportion with rise in the amount of the filler, surface coverage by particles increased from 19% for a proportion of 0.5, to 24% for a ratio of 1, and up to 48% for a ratio of 5. The cross sections show that the films were replete with the given filler, which was not surprising given the size of the DC particles observed.

The results (micrographs for PVP/p/Z + BCh) presented in **Fig. 8g-i** indicate that the BCh particles were very nearly evenly distributed throughout the polymer matrix, thereby forming random networks in the matrix. Since the space between particles decreased in line with increase in particle content, a higher BCh content formed more compact networks [50]. The comparisons presented again demonstrate that, with rise in the amount of the filler in the polymeric film, surface coverage increased from 16% for a proportion of 0.5, to 29% for a ratio of 1, and up to 63% for a ratio of 5. The cross sections show that the given fillers were evenly distributed throughout the thickness of the films. The fullest (cross-sectional) sample is black in colour, with small pale spots (unfilled spaces).

Findings resulting from the microscopic observation proved that the mechanical properties of the films were contingent not only on particle size and distribution, but also on the shape of the particles. This could also account for the deterioration in mechanical properties since the transfer of stress from the matrix to the DC type filler was less effective.

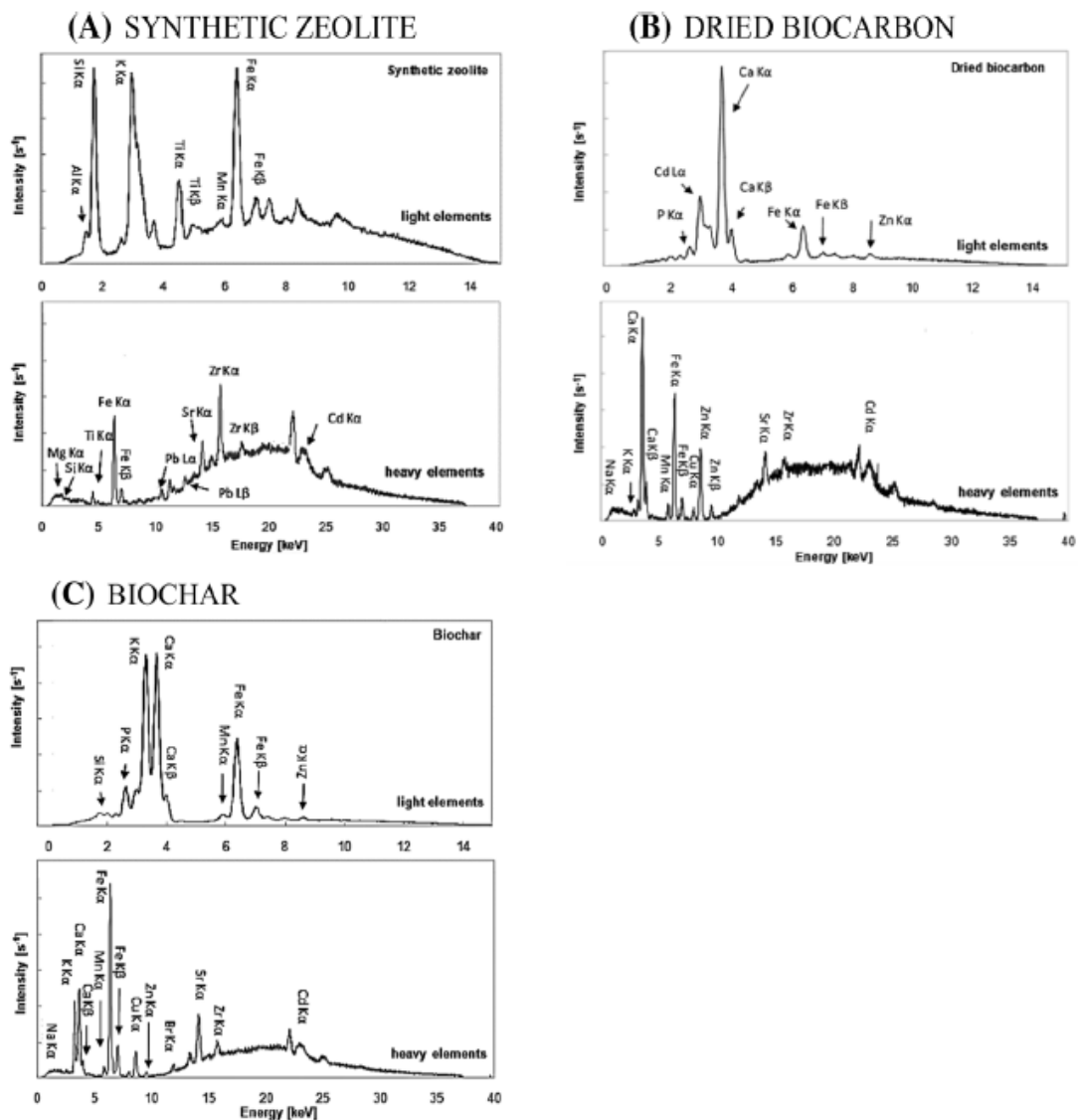


Fig. 9 XRF spectra of the fillers

Screening plant growth test (*Sinapis alba*)

The final experiment tested the effect of the polymeric films on the growth of *Sinapis alba* when acting as a seed carrier.

The films containing 5% of filler were chosen for this purpose, since they had the highest content of important macro- and micronutrients for plant growth, which would be released into the environment once the seed-carrying material dissolved.

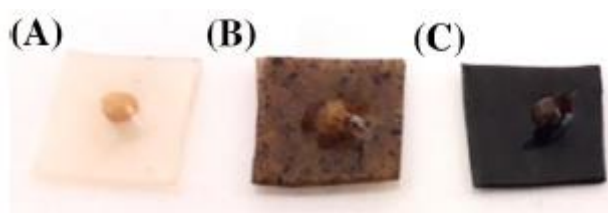


Fig. 10 *Sinapis alba* seeds encapsulated in the following polymeric films: **a** PVP/p/Z; **b** PVP/p/Z+5DC; and **c** PVP/p/Z + 5BCh

XRF analysis of the fillers (**Fig. 9**) confirmed the presence of desirable elements for planting, such as N, P, K, Ca and Mg [26]. The heightened content of Ca, Mg and K was caused by the alkaline nature of the biochar, in agreement with findings in a paper [56].

Figure 10 shows images of the prepared samples before they were planted. The seeds encapsulated in the polymeric films were placed in the soil, and their growth pattern was monitored for a period of 12 days. The first positive result was the fact that all the seeds under study, comprising 10 in total, germinated.

Table 3 displays the experimental results—the lengths of roots, heights of the plants, fresh weight at the end of experiment and RGR_{ger} and RGR_{FW} for the individual samples, wherein comparison is made with control specimens, i.e. seeds not mounted in a polymeric film. The control plants started to grow first, while the “polymeric samples” (with an encapsulated seed) showed slightly delayed growth due to the time it took the polymeric films to dissolve. The plants growing in the presence of the synthetic zeolite reached the second to highest length in the stem but had the shortest roots. None of the plants was significantly longer than the control specimens. The longest roots were discerned for those grown from polymeric films supplemented with the BCh. The polymeric films with the DC filler demonstrated slightly longer stems and shorter roots than the control plants.

The agricultural definition of rate of growth is the height of a plant at an early stage of growth, expressed as the relative growth rate of germination (RGR_{ger}). The highest recorded herein was for the polymeric films containing 5% DC, followed sequentially by: 5DC/Z > 5BCh/Z > control. This indicates that a polymeric film supplemented with DC has the potential to positively affect the initial stage of plant growth, probably due to the more rapid release of the macro- and micronutrients from the DC. The RGR_{FW} for each film, based on gain in fresh weight of the biomass evaluated at the close of the experiment, did not differ from the control significantly. This is positive, since the PVP-based polymeric films were evidently not going to inhibit further growth of the *Sinapis alba* plants.

The potential of the plants to take up elements from the polymeric films was studied by AAS. Such evaluation is related to the control specimens that could only draw upon elements from the soil environment. The results obtained are given in **Table 4**.

The first aspect was the decrease observed in the plants of most elements that grew from the material solely containing the synthetic zeolite, while the content of Na and K in them exceeded that of the control, probably through the properties for ion exchange of the zeolite.

Table 3 Selected biometric parameters for the plants at the end of the screening experiment on *Sinapis alba*, and their change in relation to the control plants (n = 10, average \pm standard deviation)

Sample	Fresh weight (mg)	Length of roots (cm)	Plant height (cm)	RGR _{ger} (cm cm ⁻¹ d ⁻¹)	RGR _{FW} (mg mg ⁻¹ d ⁻¹)
Control	108.5 \pm 27.6	3.7 \pm 2.5	6.0 \pm 1.1	0.55 \pm 0.27	0.388 \pm 0.022
PVP/p/Z	105.7 \pm 22.5	1.5 \pm 0.3	7.2 \pm 0.8	1.71 \pm 0.94	0.387 \pm 0.017
PVP/p/Z + 5DC	155.6 \pm 26.1	2.4 \pm 0.9	7.4 \pm 1.0	3.36 \pm 0.46	0.419 \pm 0.014
PVP/p/Z + 5BCh	129.5 \pm 27.4	4.3 \pm 2.3	6.7 \pm 1.0	2.05 \pm 0.76	0.394 \pm 0.032

Table 4 Accumulation of individual elements (mg/kg dry matter) in the biomass of *Sinapis alba* seedlings (n = 3, average \pm standard deviation)

	Mg (mg.kg ⁻¹)	Mn (mg.kg ⁻¹)	Na (mg.kg ⁻¹)	Zn (mg.kg ⁻¹)	K (mg.kg ⁻¹)	Ca (mg.kg ⁻¹)	Fe (mg.kg ⁻¹)
Marschner P. [46]	2000	50	–	20	10,000	5000	100
Control	2810 \pm 37	342 \pm 4	4083 \pm 8	294.7 \pm 0.8	25,773 \pm 45	877 \pm 7	3362 \pm 13
PVP/p/Z	2846 \pm 132	223 \pm 3	5633 \pm 35	308.5 \pm 6.5	36,102 \pm 90	810 \pm 16	3271 \pm 18
PVP/p/Z/5DC	2136 \pm 101	328 \pm 2	4132 \pm 23	286.3 \pm 3.5	23,799 \pm 53	495 \pm 4	3039 \pm 2
PVP/p/Z/5BCh	2301 \pm 80	317 \pm 2	3770 \pm 51	438.0 \pm 9.0	22,733 \pm 15	561 \pm 14	3555 \pm 7

It was also found that the plants growing from the films with BCh possessed a higher content of Zn and Fe, which participate in the synthesis of chlorophyll and in photosynthetic electron transport [57]. As for promotion of plant growth, biochar appeared to be more effective than the dried biocarbon, as biochar-originating elements were likely to have been more readily available. **Table 4** displays mean values of concentration for mineral elements present in dry plant shoot matter sufficient for adequate growth [58]. It can be seen that the required limits were fulfilled except for Ca. A study in the literature [57] suggests that significant decrease in Ca in plants may cause excessive accumulation of Zn.

Based on the findings reported, the authors believe that the higher presence of macronutrients stemming from the fillers, e.g. Mg and K, probably promoted the growth of the above-ground parts of the plants, while the higher accumulation of micronutrients sourced from the fillers, such as Zn and Fe, could have encouraged root growth.

Overall, it may be stated that the fillers had a positive effect on the growth of *Sinapis alba* at an early stage, and the polymer matrix of the film did not inhibit later development of the plant; however, further experiments are necessary to arrive at more precise conclusions.

Conclusion

Based on the results obtained, it can be concluded that a combination of the synthetic zeolite (prepared from the waste kaolin) and biocarbon (whether in dried form or as biochar) shows great potential as a filler for a polymeric film. Here is a summary of the findings:

- The processing and mechanical properties of the prepared polymeric films were acceptable.
- The water solubility and water uptake of the films were both satisfactory in terms of handling and any further utilization of the films.
- The results of respirometric tests indicated the beneficial effect of the biocarbon on the biodegradation of the tested films.
- The proposed combination of fillers (synthetic zeolite/biocarbon) had a positive effect on the growth of *Sinapis alba* at the initial stage, and the polymer matrix of the PVP film did not inhibit further development of the plant.

Based on these observations and from testing the processing and mechanical properties of the polymeric films, it can be concluded that the environmentally friendly polymeric film, based on PVP with different combinations of filler (synthetic zeolite/biocarbon), could be utilized in agro-chemistry.

References

1. Hopewell J, Dvorak R, Kosior E (2009) Plastics recycling: challenges and opportunities. *Phil Trans R Soc B* 364(1526):2115-2126. <https://doi.org/10.1098/rstb.2008.0311>
2. Faruk O, Bledzki AK, Fink HP, Sain M (2012) Biocomposites reinforced with natural fibers: 2000-2010. *Prog Polym Sci* 37(11):1552-1596. <https://doi.org/10.1016/j.progpolymsci.2012.04.003>
3. Jawaid M, Sapuan SM, Allothman OY (eds) (2016) Green biocomposites: manufacturing and properties. Springer, Berlin. <https://doi.org/10.1007/978-3-319-46610-1>
4. Mohanty JR, Das SN, Das HC, Swain SK (2014) Effect of chemically modified date palm leaf fiber on mechanical, thermal and rheological properties of polyvinylpyrrolidone. *Fiber Polym* 15(5):1062-1070. <https://doi.org/10.1007/s12221-014-1062-6>
5. Nešić A, Ružić J, Gordić M, Ostojić S, Micić D, Onjia A (2017) Pectin-polyvinylpyrrolidone films: a sustainable approach to the development of biobased packaging materials. *Compos Part B-Eng* 110:56-61. <https://doi.org/10.1016/j.compositesb.2016.11.016>
6. Acton QA (2013) Polyvinyls-advances in research and application. Scholarly Editions, Georgia
7. O'Haire T, Russell SJ, Carr ChM (2016) Centrifugal melt spinning of polyvinylpyrrolidone (PVP)/triacetene copolymer fibres. *J Mater Sci* 51 (16):7512-7522. <https://doi.org/10.1007/s10853-016-0030-5>
8. Vieira MGA, Silva MA, Santos LO, Beppu MM (2011) Natural-based plasticizers and biopolymer films: a review. *Eur Polym J* 47(3):254-263. <https://doi.org/10.1016/j.eurpolymj.2010.22.011>
9. Arfat YA (2017) Plasticizers for biopolymer films. In: Ahmed J (ed) *Glass transition and phase transitions in food and biological materials*. John Wiley, Chichester, p 2017
10. Roy N, Saha N, Kitano T, Saha P (2012) Biodegradation of PVP-CMC hydrogel film: a useful food packaging material. *Carbohydr Polym* 89(2):346-353. <https://doi.org/10.1016/j.carbpol.2012.03.008>
11. Chapi S, Devendrappa H (2016) Optical, electrical, thermal and electrochemical studies of spin-coated polyblend-ZnO nanocomposites. *J Mater Sci: Mater Electron* 27:11974-11985. <https://doi.org/10.1007/s10854-016-5344-1>

12. Mohamed AM, Osman MH, Smaoui H, Ariffin MAM (2017) Permeability and tensile strength of concrete with arabic gum biopolymer. *Adv Civ Eng* 2017:1-7. <https://doi.org/10.1155/2017/4703841>
13. Allison PG, Moser RD, Chandler MQ, Caminero-Rodriguez JA, Torres-Cancel K, Rivera OG, Goodwin JR, Gore ER, Weiss CA (2015) Mechanical, thermal, and microstructural analysis of polyvinyl alcohol/montmorillonite nanocomposites. *J Nanomater* 2015:9. <https://doi.org/10.1155/2015/291248>
14. Babaladimath G, Chapi S (2018) Microwave-assisted synthesis, characterization of electrical conducting and electrochemical xanthan gum-graft-polyaniline. *J Mater Sci: Mater Electron* 29:1115911166. <https://doi.org/10.1007/s10854-018-9201-2>
15. Chapi S (2020) Optical, electrical and electrochemical properties of PCL5/ITO transparent conductive films deposited by spin-coating-Materials for single-layer devices. *J Sci-Adv Mater Dev* 5(3):322-329. <https://doi.org/10.1016/j.jsamd.2020.07.005>
16. Chapi S (2021) Influence of Co²⁺ on the structure, conductivity, and electrochemical stability of poly(ethylene oxide)-based solid polymer electrolytes: energy storage devices. *J Elec Mater* 50:15581571. <https://doi.org/10.1007/s11664-020-08706-6>
17. Rodriguez-Castellanos W, Rodrigue D (2016) Production and characterization of hybrid polymer composites based on natural fibers. In: Poletto M (ed) *Composites from renewable and sustainable materials*. Rijeka, Intech, pp 273-302. <https://doi.org/10.5772/64995>
18. Alver E, Metin AU, Ciftci H (2014) Synthesis and characterization of chitosan/polyvinylpyrrolidone/ zeolite composite by solution blending method. *J Inorg Organomet Polym* 24:1048-1054. <https://doi.org/10.1007/s10904-014-0087-z>
19. Zhang Q, Cai H, Yang K, Yi W (2017) Study of the preparation and properties of biochar/ plastic composites. *Results Phys* 7:2391-2395. <https://doi.org/10.1016/j.rinp.2017.04.025>
20. Behazin E, Misra M, Mohanty AK (2017) Sustainable biocarbon from pyrolyzed perennial grasses and their effects on impact modified polypropylene biocomposites. *Compos Part B-Eng* 118:116-124. <https://doi.org/10.1021/acsomega.7b00122>
21. Mashouf Roudsari G, Misra M, Mohanty AK (2017) A statistical approach to develop biocomposites from epoxy resin, poly(furfuryl alcohol), poly(propylene carbonate), and biochar. *J Appl Polym Sci* 134(38):45307. <https://doi.org/10.1002/app.45307>
22. Nan N, DeVallance DB, Xie X, Wang J (2016) The effect of bio-carbon addition on the electrical, mechanical, and thermal properties of polyvinyl alcohol/biochar composites. *J Compos Mater* 50(9):1161-1168. <https://doi.org/10.1177/0021998315589770>
23. Das O, Bhattacharyya D, Hui D, Lau KT (2016) Mechanical and flammability characterisations of bio-char/polypropylene biocomposites. *Compos Part B-Eng* 106:120-128. <https://doi.org/10.1016/j.compositesb.2016.09.020>
24. Giorcelli M, Bartoli M (2019) Development of coffee biochar filler for the production of electrical conductive reinforced plastic. *Polymers* 11(12):1916. <https://doi.org/10.3390/polym11121916>

25. Raya-Moreno I, Cañizares R, Domene X (2017) Comparing current chemical methods to assess biochar organic carbon in a Mediterranean agricultural soil amended with two different biochars. *Sci Total Environ* 598:604-615. <https://doi.org/10.1016/j.scitotenv.2017.03.168>
26. Uzoma K, Inoue M, Andry H, Fujimaki H, Zahoor A (2011) Effect of cow manure biochar on maize productivity under sandy soil condition. *Soil Use Manage* 27:205-212. <https://doi.org/10.1111/j.1475-2743.2011.00340.x>
27. Chen S, Ming Y, Chuang B, Susu Y, Yifei J, Hongtao Z, Yulong Z (2018) Preparation and characterization of slow-release fertilizer encapsulated by biochar-based waterborne copolymers. *Sci Total Environ* 615:431-437. <https://doi.org/10.1016/j.scitotenv.2017.09.209>
28. Jurča M, Julinová M, Slavík R (2019) Negative effect of clay fillers on the polyvinyl alcohol biodegradation. *Sci Eng Compos Mater* 26(1):97-103. <https://doi.org/10.1515/secm-2017-0202>
29. Asaithambi B, Ganesan GS, Kumar SA (2017) Banana/sisal fibers reinforced poly(lactic acid) hybrid biocomposites; influence of chemical modification of BSF towards thermal properties. *Polym Compos* 38(6):1053-1062. <https://doi.org/10.1002/pc.23668>
30. Wanderson F, Ribeiro M, Ryan L, Kotzebue V (2017) Thermal and mechanical analyses of biocomposites from cardanol-based polybenzoxazine and bamboo fibers. *J Therm Anal Calorim* 129:281-289. <https://doi.org/10.1007/s10973-017-6191-x>
31. Baba BO, Ozmen U (2015) Preparation and mechanical characterization of chicken feather/PLA composites. *Polym Compos* 38(5):837-845. <https://doi.org/10.1002/pc.23644>
32. Baba BO, Ozmen U (2017) Thermal characterization of chicken feather/PLA biocomposites. *J Therm Anal Calorim* 129:347-355. <https://doi.org/10.1007/s10973-017-6188-5>
33. Reddy TRK, Rao TS, Suvarna RP, Kumar MA (2013) Prediction on tensile properties of cow dung powder filled glass-polyester hybrid composites. *IEEE Conf Ser* 2013:702-705
34. Eze U, Ishidi E, Uche C, Madufor I (2016) Effect of maleic anhydride graft-polyethylene (MAPE) on mechanical properties of cow dung and poultry dung filled low density polyethylene (LDPE) composites. *Int J Innov Environ Stud Res* 4(1):19-27
35. Yusefi M, Khalid M, Yasin FM, Abdullah LC, Ketabchi MR, Walvekar R (2018) Performance of cow dung reinforced biodegradable poly(lactic acid) biocomposites for structural applications. *J Polym Environ* 26(2):474-486. <https://doi.org/10.1007/s10924-017-0963-z>
36. Dixit S (2014) Degradation analysis of lignocellulosic fillers infused coir epoxy composites in different environmental conditions. *Int J Lignocellul Prod* 1(2):160-179. <https://doi.org/10.22069/IJLP.2014.2073>
37. Raghuwanshi S, Negi H, Aggarwal T (2015) Comparative biodegradation studies of cow dung modified epoxy with epoxy using an indigenously developed bacterial consortium. *Afr J Microbiol Res* 9(24):1558-1572. <https://doi.org/10.5897/AJMR2015.7462>
38. Khalid M, Ratnam CT, Abdullah LC, Walvekar R, Ching YC, Ketbchi MR (2016) Mechanical and physical performance of cow dung-based polypropylene biocomposites. *Polym Compos* 39(1):288-296. <https://doi.org/10.1002/pc.23928>

39. Roy K, Akhtar A, Schlev SD, Hsu M (2017) Development and characterization of novel biochar-mortar composite utilizing waste derived pyrolysis biochar. *Int J Sci Eng Res* 8(12):1912-1919
40. ISO 15705 (2002) Water quality - Determination of the chemical oxygen demand - Small-scale dealer-tube method
41. Julinová M, Slavík R, Vyoralová M, Kalendová A, Alexy P (2018) Utilization of waste lignin and hydrolysate from chromium tanned waste in blends of hot-melt extruded PVA-starch. *J Polym Environ* 26(4):1459-1472. <https://doi.org/10.1007/s10924-017-1050-1>
42. Costa P, Lobo JMS (2001) Modeling and comparison of dissolution profiles. *Eur J Pharm Sci* 13(2):123-133. [https://doi.org/10.1016/S0928-0987\(01\)00095-1](https://doi.org/10.1016/S0928-0987(01)00095-1)
43. Julinová M, Kupec J, Alexy P, Hoffmann J, Sedlařík V, Vojtek T, Chromčáková J, Bugaj P (2010) Lignin and starch as potential inductors for biodegradation of films based on poly (vinyl alcohol) and protein hydrolysate. *Polym Degrad Stab* 95(2):225-233. <https://doi.org/10.1016/j.polymdegradstab.2009.10.008>
44. ISO 11269-2 (2013) Soil quality - Determination of the effects of pollutants on soil flora - Part 2: Effects of chemicals on the emergence and growth of higher plants
45. Tripathi S, Bhadouria R, Srivastava P, Devi RS, Chaturvedi R, Raghubanshi AS (2020) Effects of light availability on leaf attributes and seedling growth of four tree species in tropical dry forest. *Ecol Process* 9(1):1-16. <https://doi.org/10.1186/s13717-019-0206-4>
46. Naskar MK, Kundu D, Chatterjee M (2011) Influence of PVP buffer layer on the formation of NaA zeolite membrane. *J Porous Mater* 18(3):319-327. <https://doi.org/10.1007/s10934-010-9381-5>
47. Sionkowska A (2003) Interaction of collagen and poly (vinyl pyrrolidone) in blends. *Eur Polym J* 39(11):2135-2140. [https://doi.org/10.1016/S0014-3057\(03\)00161-7](https://doi.org/10.1016/S0014-3057(03)00161-7)
48. Liu Y, Yan C, Zhao J, Zhang Z, Wang H, Zhou S, Wu L (2018) Synthesis of zeolite P1 from fly ash under solvent-free conditions for ammonium removal from water. *J Clean Prod* 202:11-22. <https://doi.org/10.1016/j.jclepro.2018.08.128>
49. Cantrell KB, Hunt PG, Uchimiya M, Novak JM, Ro KS (2012) Impact of pyrolysis temperature and manure source on physicochemical characteristics of biochar. *Bioresour Technol* 107:419-428. <https://doi.org/10.1016/j.biortech.2011.11.084>
50. Nagarajan V, Mohanty AK, Misra M (2016) Biocomposites with size-fractionated biocarbon: influence of the microstructure on macroscopic properties. *ACS Omega* 1(4):636-647. <https://doi.org/10.1021/acsomega.6b00175>
51. Mahmoudi Beram F, Koohmareh GA, Malekpour A (2019) Preparation and characterization of aqueous stable electro-spun nanofibers using polyvinyl alcohol/polyvinyl pyrrolidone/zeolite. *Soft Mater* 17(1):41-56. <https://doi.org/10.1080/1539445X.2018.1546191>
52. Saroj AL, Singh RK, Chandra S (2013) Studies on polymer electrolyte poly (vinyl) pyrrolidone (PVP) complexed with ionic liquid: effect of complexation on thermal stability, conductivity and relaxation behaviour. *Mater Sci Eng B* 178(4):231-238. <https://doi.org/10.1016/j.mseb.2012.11.007>
53. Wypych G (2011) Handbook of polymers. Chem Tec Publishing, Canada, p 2011

54. Bennet GM (2016) Seed inoculation, coating and precision pelleting: science technology and practical applications. CRC Press, USA
55. Meena RS, Das A, Yadav GS, Lal R (2018) Legumes for soil health and sustainable management. Springer, India
56. Huang WJ (2017) Engineering applications of biochar. InTech, Croatia
57. Zhao H, Wu L, Chai T, Zhang Y, Tan J, Ma S (2012) The effects of copper, manganese and zinc on plant growth and elemental accumulation in the manganese-hyperaccumulator *Phytolacca americana*. J Plant Physiol 169:1243-1252. <https://doi.org/10.1016/j.jplph.2012.04.016>
58. Marschner's MP (2012) Mineral nutrition of higher plants. Elsevier, Australia